

Supplemental Information – Caron et al.

Supplemental Movies

Supplemental Movie S1. Time lapse video of hESC-derived myoblasts proliferating, aligning and fusing together into myotubes, related to Figure 1.

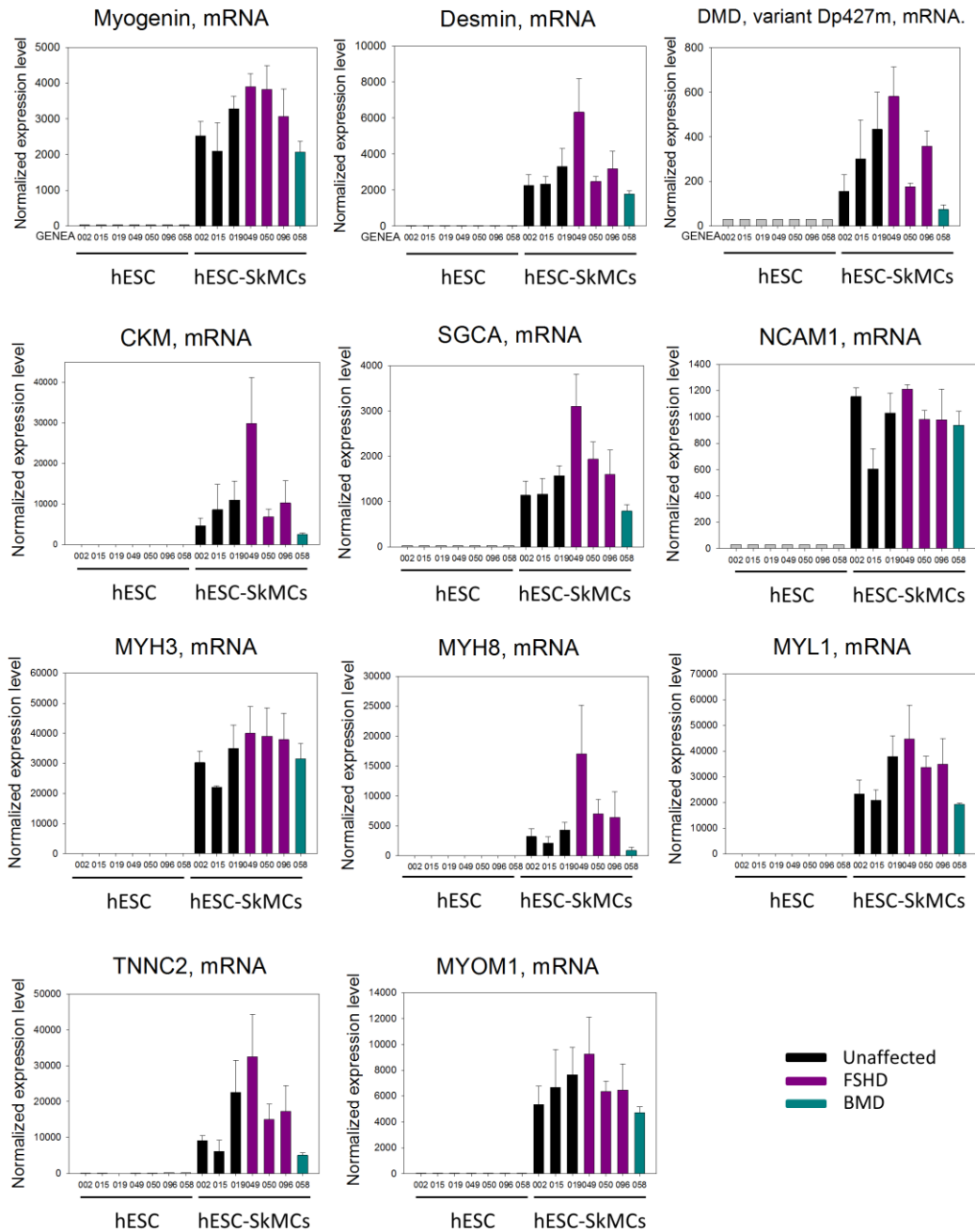
GERI Time-lapse incubator (GeneaBiomedx.com) was used to generate the video.

Differentiating hESC were incubated from d14 to d26 into GERI incubator. Time lapse images were taken at one image every 5 min. Images were sequenced together using python script and the open source software virtual dub was used to create a video file.

Supplemental Movie S2. Time lapse video of contracting hESC-myotubes.

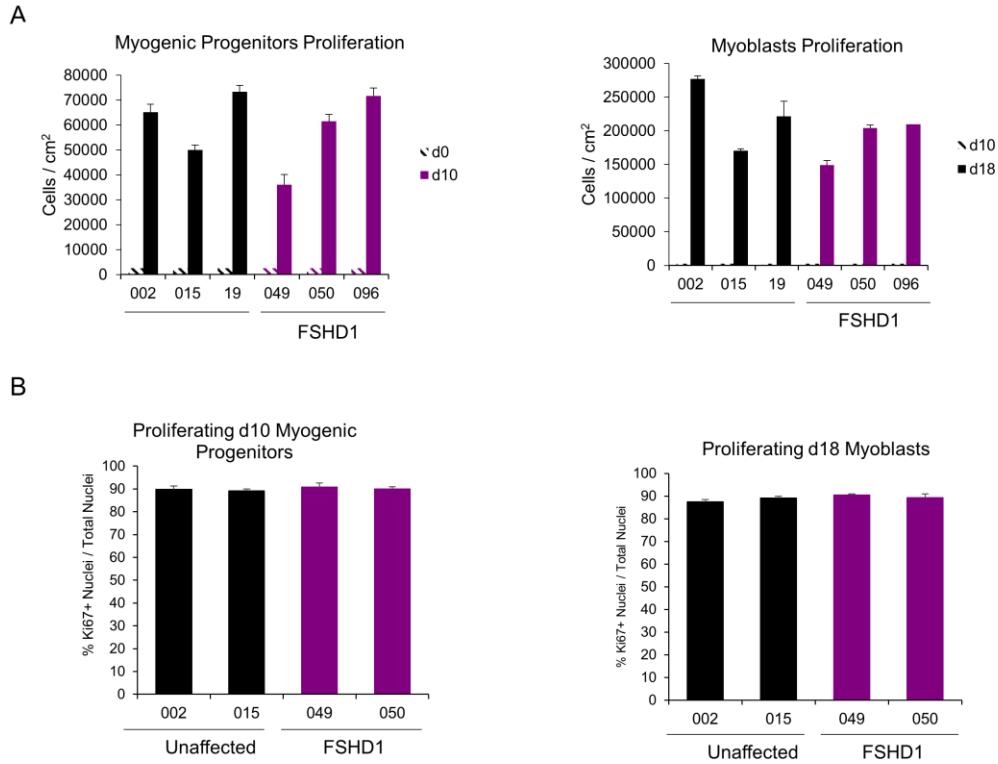
Infinity Capture Software (Lumenera Corporation) was used to capture avi. files and generate the video.

Supplemental Figures



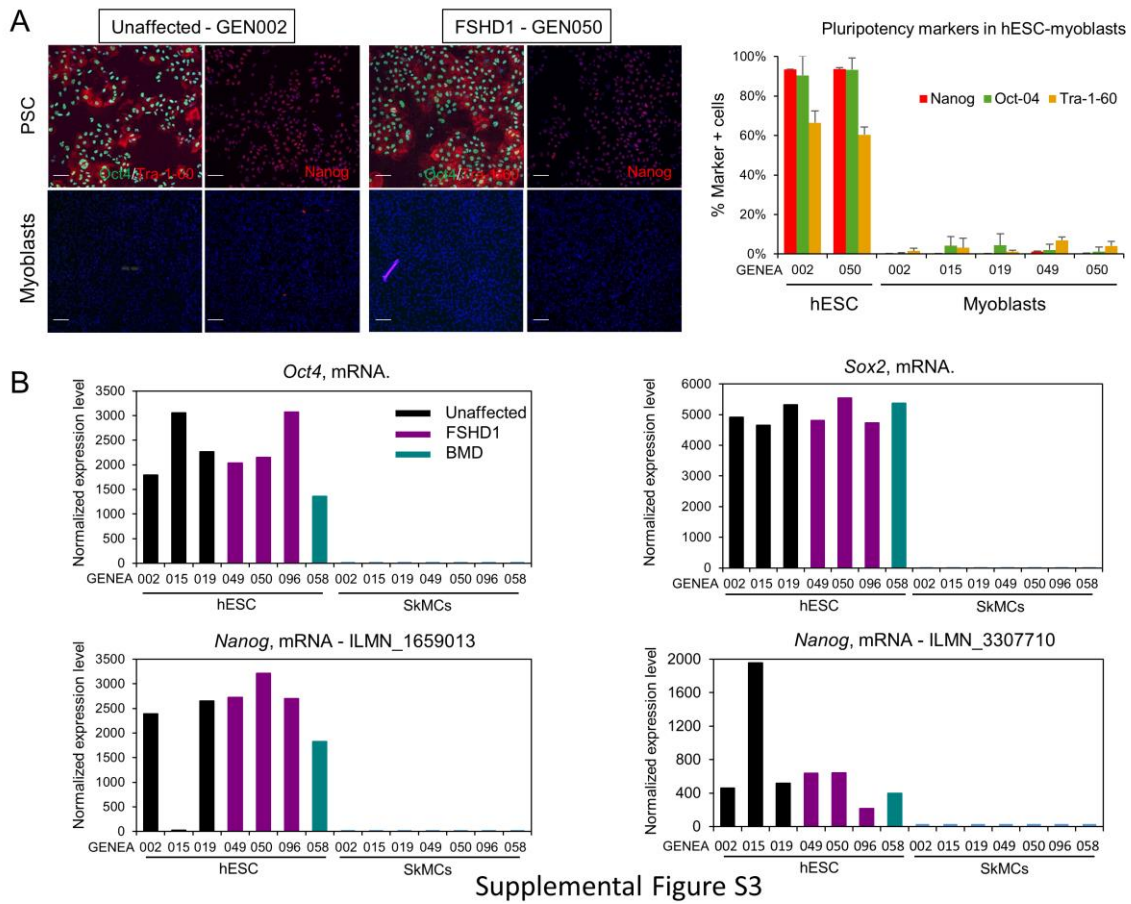
Supplemental Figure S1

Figure S1. Skeletal muscle specific genes expression obtained from the microarray analysis of hESC-myotubes at d26. Diagrams represent the normalized expression level of specific mRNA in three unaffected, three FSHD1 and one BMD hESC lines. Error bars represent the SEM of three biological replicates.



Supplemental Figure S2

Figure S2. Proliferation of myogenic progenitors and myoblasts of unaffected and FSHD1 affected hESC lines. (A) Number of myogenic progenitors and myoblasts generated from three control and three FSHD1 hESC lines. For myogenic progenitors, cells were plated at 2630 cells/cm² at d0 and counted at d10. For myoblasts, cells were plated at 2630 cells/cm² at d10 and counted at d18. (B) Ki67 staining quantification at the myogenic progenitor and myoblast stages in two unaffected and two FSHD1-hESC lines.



Oct4, mRNA.

Cell Type	GENEA	Unaffected	FSHD1	BMD
hESC	002	~1800	~3100	~2300
	015	~1800	~3100	~2300
	019	~1800	~3100	~2300
	049	~1800	~3100	~2300
	050	~1800	~3100	~2300
	096	~1800	~3100	~2300
SkMCs	058	~1400	~1400	~1400

Sox2, mRNA.

Cell Type	GENEA	Unaffected	FSHD1	BMD
hESC	002	~4800	~5500	~4800
	015	~4800	~5500	~4800
	019	~4800	~5500	~4800
	049	~4800	~5500	~4800
	050	~4800	~5500	~4800
	096	~4800	~5500	~4800
SkMCs	058	~5500	~5500	~5500

Nanog, mRNA - ILMN_1659013

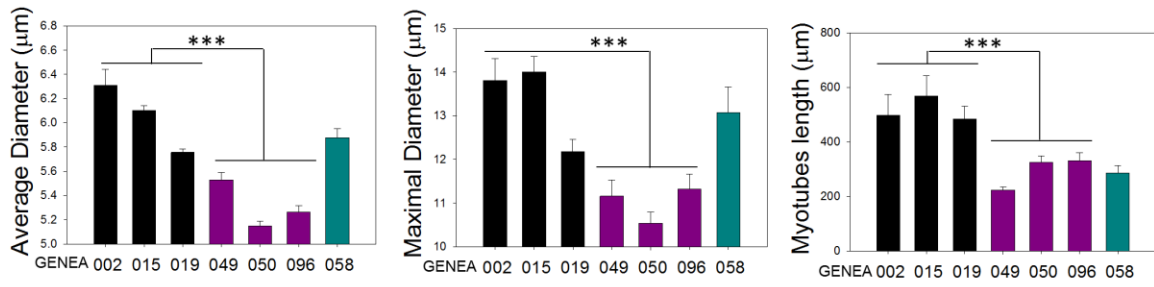
Cell Type	GENEA	Unaffected	FSHD1	BMD
hESC	002	~2400	~3200	~2600
	015	~2400	~3200	~2600
	019	~2400	~3200	~2600
	049	~2400	~3200	~2600
	050	~2400	~3200	~2600
	096	~2400	~3200	~2600
SkMCs	058	~1800	~1800	~1800

Nanog, mRNA - ILMN_3307710

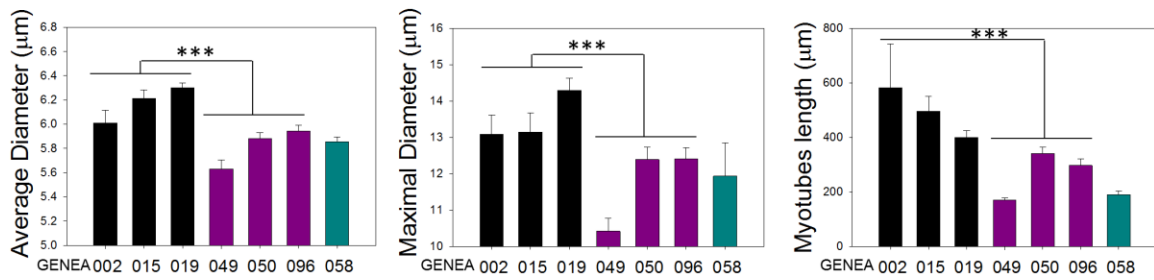
Cell Type	GENEA	Unaffected	FSHD1	BMD
hESC	002	~400	~1900	~500
	015	~400	~1900	~500
	019	~400	~1900	~500
	049	~400	~1900	~500
	050	~400	~1900	~500
	096	~400	~1900	~500
SkMCs	058	~400	~400	~400

Figure S3. Pluripotency markers analysis in hESC-myoblasts and myotubes. (A) Images of pluripotency markers staining in undifferentiated hESC and myoblasts derived from unaffected control and FSHD1-affected hESC lines. Scale bars = 100 μ m. The graph on the right represents the quantification of the staining. (B) Pluripotency markers mRNA expression from the microarray analysis of hESC-myotubes. Diagrams represent the normalized expression level of specific mRNA in three unaffected, three FSHD1 and one BMD hESC lines. Error bars represent the SEM of three biological replicates.

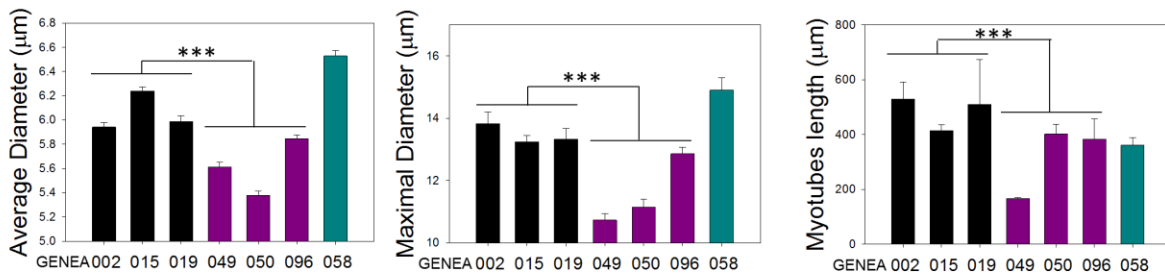
Experiment 1



Experiment 2



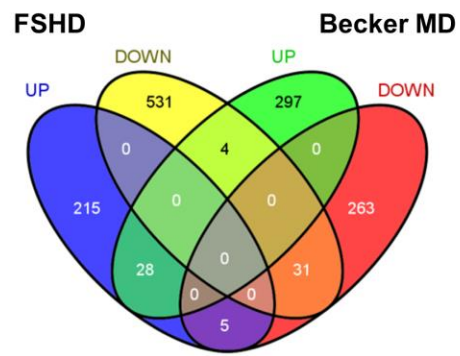
Experiment 3



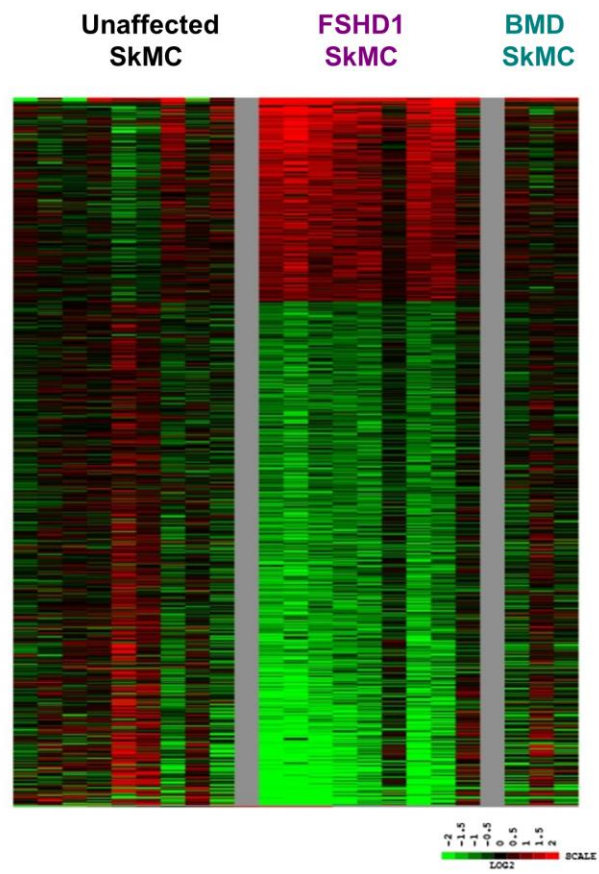
Supplemental Figure S4

Figure S4. HESC-myotubes morphology analysis of each independent experiment. Diagrams represent the mean values +/- 99% confidence. Statistical analysis was performed between the mean value of 12 fields (***) $p < 0.001$.

A

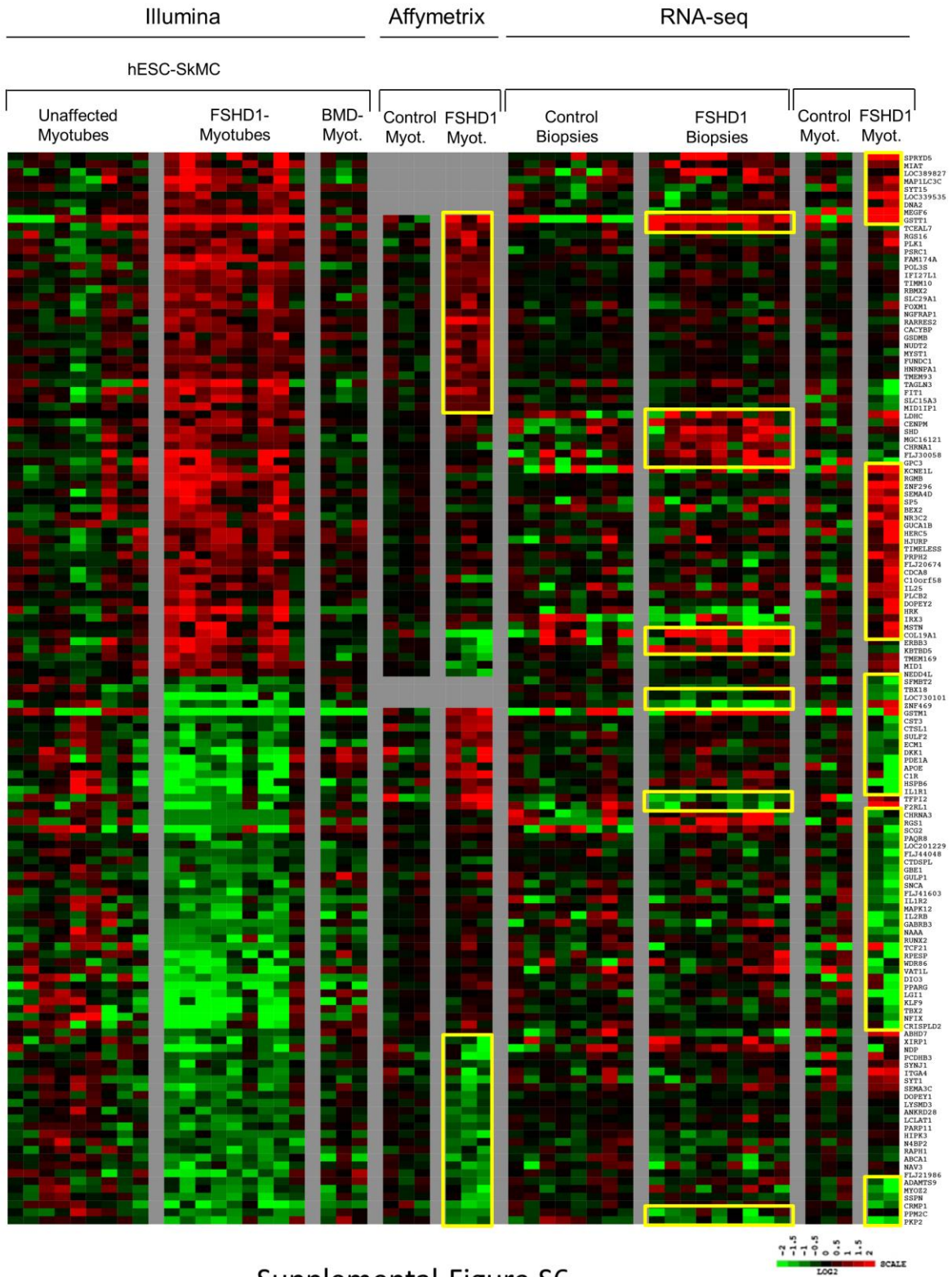


B



Supplemental Figure S5

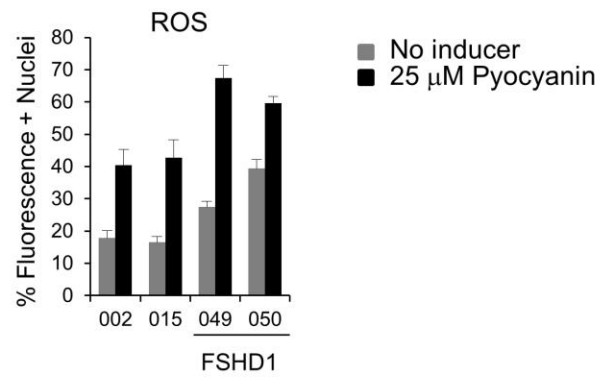
Figure S5. (A) Venndiagram showing FSHD-specific gene dysregulation in FSHD-myotubes versus unaffected and BMD-affected controls. (B) Heatmap showing FSHD-specific gene expression profile in FSHD-myotubes versus unaffected and BMD-affected controls. Gene probe sets with minimum 1.5- fold change (on a Log2 scale) and t-test significance $P < 0.05$ on the average of FSHD1 or BMD samples over the average of the unaffected controls were isolated.



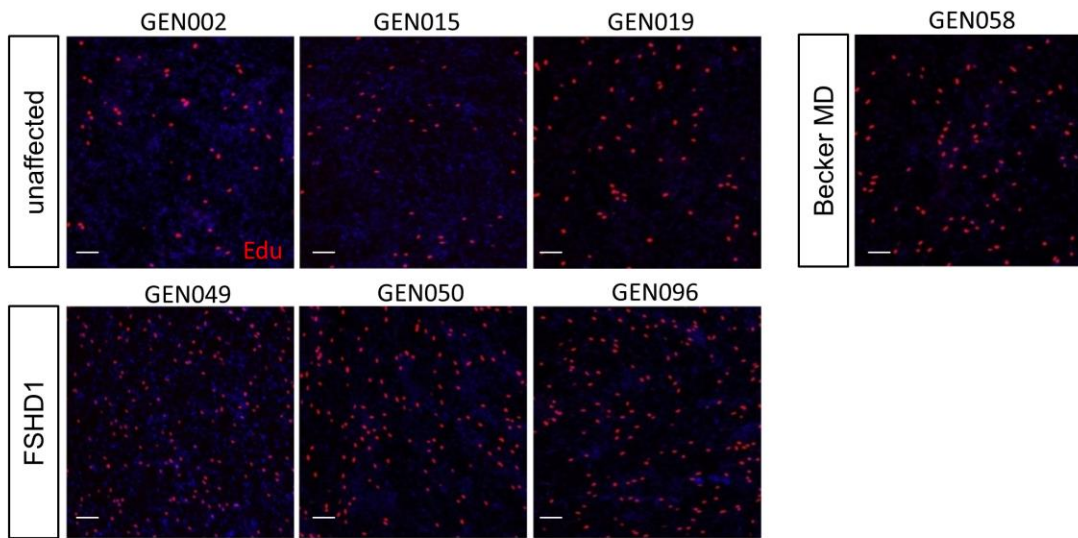
Supplemental Figure S6

Figure S6. Comparative heatmap showing the 137 FSHD1-dysregulated genes of our Illumina microarray analysis that are common to Yao et al. RNA-seq study and/or Tsumagari et al. Affymetrix microarray analysis. Target genes that show >1.5 fold-change between the average of the FSHD1 versus control samples in the RNA-Seq and/or Affymetrix datasets in agreement with the Illumina data were identified. The RNA-Seq data excludes sample C6 for the Yao et al. dataset due to low sequencing depth. A selection of the target genes that are in agreement with the Illumina data have been boxed up in yellow.

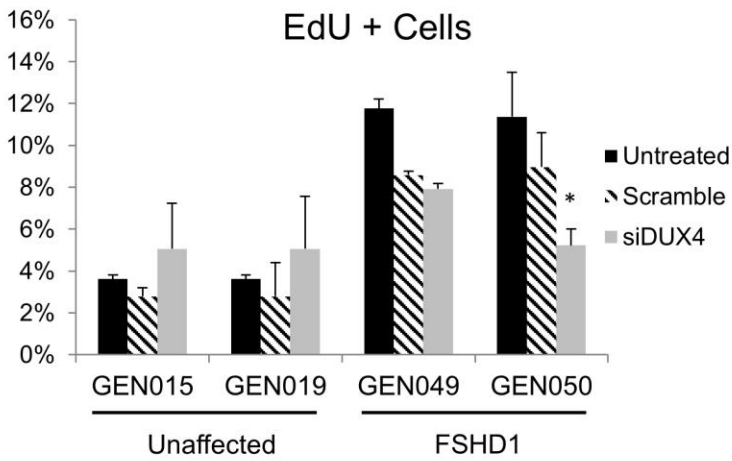
A



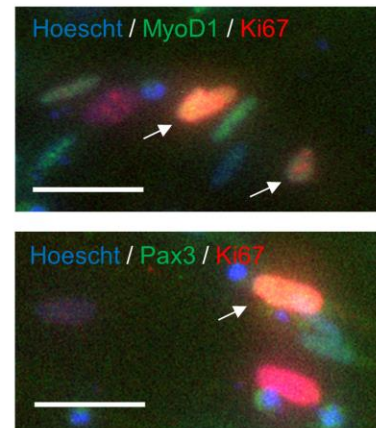
B



C

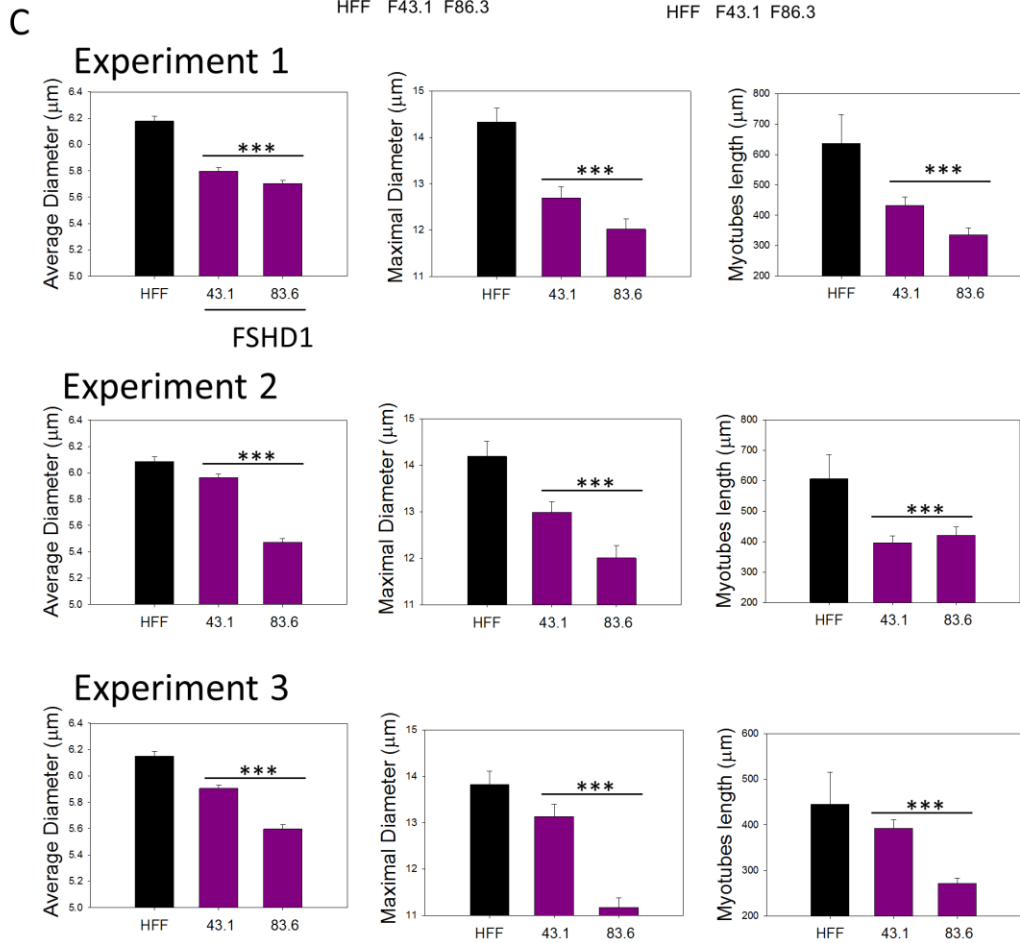
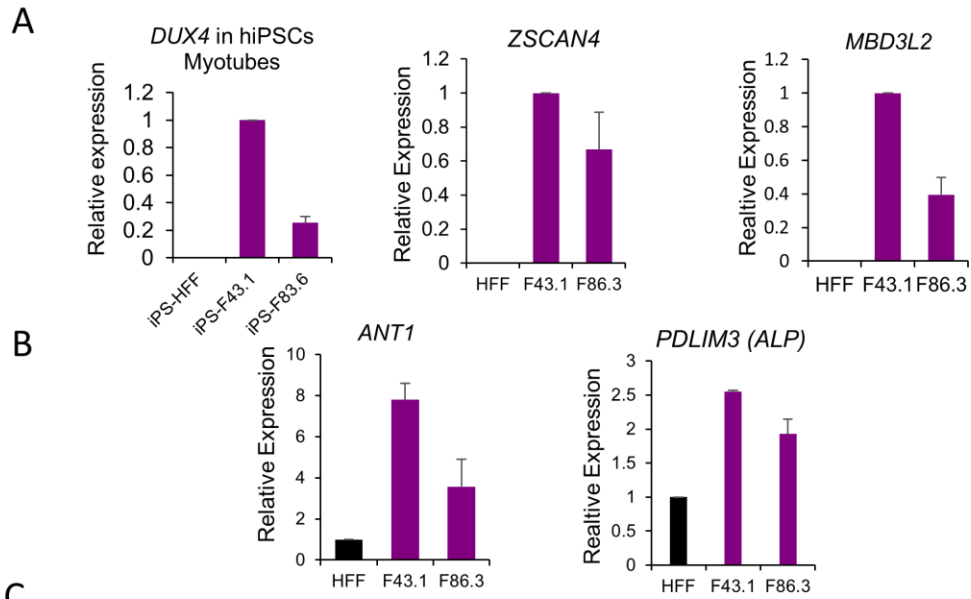


D



Supplemental Figure S7

Figure S7. ROS detection and cell proliferation assay in hESC-derived SkMCs. (A) Quantitative analysis of green fluorescence positive cells in myotubes culture after 30 minutes treatment with or without 25 μ M pyocyanin. (B) Immunofluorescence images of EdU staining in myotube cultures derived from three unaffected, three FSHD1 and one BMD affected hESC lines. Scale bars = 100 μ m. (C) Quantitative analysis of EdU positive cells in myotube cultures transfected with DUX4 siRNA or scramble. Diagrams represent the mean values +/- SEM. (D) Immunofluorescence images of co-immunostaining of MYOD1/Ki67 or PAX3/Ki67 in hESC-myotube cultures. Scale bars = 50 μ m.



Supplemental Figure S8

Figure S8. (A) qPCR analysis of *DUX4*, *ZSCAN4*, *MBD3L2* expression in hiPSC-myotubes. (B) qPCR analysis of *ANT1* and *PDLIM3* in hiPSC-myotubes. RNA was harvested from one unaffected and two FSHD1-affected hiPSC lines after 26 days skeletal muscle differentiation. Ct values for *DUX4*, *ZSCAN4*, *MBD3L2*, *ANT1* and *PDLIM3* expressions were normalized to Ct values for the reference gene GAPDH. (C) HiPSC-myotubes morphology analysis (average and maximal diameter and myotube length) of each independent experiment. Diagrams represent the mean values +/- 99% confidence. Statistical analysis was performed between the mean values of 12 fields (**p<0.001).

Table S1. hESC and hiPSC properties.

Supplemental Table S1. hESC and hiPSC properties

	Cell line	Karyotype	Disease Status	Mutation	D4Z4 array size
	GENEA002	46 , XY	Unaffected	N/A	N/A
	GENEA015	46 , XY	Unaffected	N/A	N/A
	GENEA019	46 , XX	Unaffected	N/A	N/A
hESC	GENEA049*	46 , XX	FSHD1	deletion in the D4Z4 DNA region on 4q35	D4Z4 fragment of 22.6 kb
	GENEA050*	46 , XY	FSHD1	deletion in the D4Z4 DNA region on 4q35	D4Z4 fragment of 22.6 kb
	GENEA096	46 , XX	FSHD1	deletion in the D4Z4 DNA region on 4q35	D4Z4 fragment of 24 kb
	GENEA058	46, XY	Becker MD	deletion of exons 3-6 on the DMD gene on Xq21.2	N/A
	HFF-1^	46 , XY	Unaffected	N/A	N/A
hiPSC	FSHD-43.1^	46 , XY	FSHD1	deletion in the D4Z4 DNA region on 4q35	D4Z4 fragment of 20 kb
	FSHD-83.6^	46 , XX	FSHD1	deletion in the D4Z4 DNA region on 4q35	D4Z4 fragment of 15 kb

* GEN049 & GEN050 are siblings

^ hiPSC lines are described in Snider et al., 2010.

Table S2. List of FSHD-associated dysregulated genes from microarray analysis.

Supplemental Material and Methods

Cell lines derivation: Donated embryos were originally created by assisted reproduction technologies for the purpose of procreation and cultured to the blastocyst stage. Trophoectoderm biopsy and preimplantation genetic diagnosis (PGD) was performed on blastocysts at day 5 or 6, to identify embryos inheriting disease causing mutations (1). For the 3 FSHD1 cell lines, FSHD

chromosome deletion (reduction in the number of 3.3 kb tandem repeats at the 4q35 locus) cannot be tested directly via single cell PCR due to its location in a highly repetitive DNA area close to the end of chromosome 4. PGD analysis is therefore performed by STR linkage marker analysis using a combination of established familial polymorphism patterns and genome database entries to establish which chromosome ends are likely to be present in any embryo. Embryo donation, stem cell line derivation and culture were performed as previously described (2-4).

RT-qPCR:

RNA was treated with DNase in solution using Turbo DNase (Life Technologies, cat. AM1907M). Briefly, 10X DNase buffer and 2 units of DNase (1 μ l) were added to the RNA. Samples were incubated 30' at 37°C. To remove the DNase from the solution, samples were treated with the DNase Inactivation Reagent. More in details, 0.2 volumes of DNase Inactivation Reagent is added and the suspension is incubated at RT with gently mixing every 30'' for 5'. Samples are then centrifuged 1' at 10000 g at RT to spin down DNase Inactivation Reagent with bound DNase and recover the RNA solution. Pay attention not to carry over residues of DNase Inactivation Reagent as it inhibits cDNA synthesis.

After quantification, 1 μ g of RNA was retrotranscribed with Superscript III First-Strand Synthesis SuperMix for qRT-PCR (Life Technologies, cat. 11752-050). Briefly, RT reactions are incubated 10' at RT, then 40 minutes (instead than 30) at 50°C and then moved for 5' at 85°C. Next, samples are incubated on ice for 5 minutes, spinned down and RNase H is added. Then, samples are incubated 20' at 37°C.

2 μ l of cDNA is used in qPCR using the SYBR GreenER qPCR SuperMix Universal kit.

All primers (sequences below) work at 58°C. In order to allow expression analysis with the $\Delta\Delta C_T$ method, all primers were tested and selected for amplification efficiencies ranging between 90-110%.

Real-Time PCR is run on a CFX96 Bio-Rad Real-Time PCR Detection System.

The cycling program for *DUX4*, *ZSCAN4* and *MBD3L2* is the following:

- 1. 95°C 10' Initial denaturation step
- 2. 95°C 30''
- 3. 58°C 30''
- 4. 72°C 30'' go to 2 for 45 cycles
- 5. Melting curve analysis.

For the other genes, 35 cycles were used.

DUX4- F (Lemmers et al., 2010)	CCCAGGTACCAGCAGACC
DUX4- R (Lemmers et al., 2010)	TCCAGGAGATGTA ACTCTAATCCA
GAPDH- F	TCAAGAAGGTGGTGAAGCAGG
GAPDH- R	ACCAGGAAATGAGCTTGACAAA
ZSCAN4- F	GTGGCCACTGCAATGACAA
ZSCAN4- R	AGCTTCCTGTCCCTGCATGT
MBD3L2- F	CGTTCACCTCTTTTCCAAGC
MBD3L2- R	AGTCTCATGGGAGAGCAGA
GSTT1- F	TGCCGCGCTGTTTACATCTT
GSTT1- R	GTGCTGACCTTTAATCAGATCCA
Notch1- F	GAGGCGTGGCAGACTATGC
Notch1- R	CTTGTA CTCCGTCAGCGTGA
Dll1- F	GATTCTCCTGATGACCTCGCA
Dll1- R	TCCGTAGTAGTGTTTCGTCACA
ANT1- F	TGCCTACTTCGGAGTCTATGATACTG
ANT1- R	GCAATCATCCAGCTCACAAAAA
ALP-F	CTCAGGGGGCATAGACTTCA

ALP- R	ATCTCCAGGACACAGGTTGG
PITX1- F	ACATGAGCATGAGGGAGGAG
PITX1- R	GTTACGCTCGCGCTTACG
MSTN- F	TCCTCAGTAAACTTCGTCTGGA
MSTN- R	CTGCTGTCATCCCTCTGGA

Supplemental References

1. McArthur SJ, Leigh D, Marshall JT, Gee AJ, De Boer KA, Jansen RP. Blastocyst trophoctoderm biopsy and preimplantation genetic diagnosis for familial monogenic disorders and chromosomal translocations. *Prenatal diagnosis*. 2008;28(5):434-42.
2. Peura T, Bosman A, Chami O, Jansen RP, Texlova K, Stojanov T. Karyotypically normal and abnormal human embryonic stem cell lines derived from PGD-analyzed embryos. *Cloning and stem cells*. 2008;10(2):203-16.
3. Peura TT, Schaft J, Stojanov T. Derivation of human embryonic stem cell lines from vitrified human embryos. *Methods in molecular biology (Clifton, NJ)*. 2010;584:21-54.
4. Bradley CK, Peura T, Dumevska B, Jovasevic A, Chami O, Schmidt U, et al. Cell lines from morphologically abnormal discarded IVF embryos are typically euploid and unaccompanied by intrachromosomal aberrations. *Reproductive biomedicine online*. 2014;28(6):780-8.